Catalysis Today 164 (2011) 257–261

Contents lists available at ScienceDirect

Catalysis Today

journal homepage: www.elsevier.com/locate/cattod

Hydrogen production by steam reforming of acetic acid over Ni-based catalysts

Somsak Thaicharoensutcharittham[a], Vissanu Meeyoo[b,*], Boonyarach Kitiyanan[a], Pramoch Rangsunvigit[a], Thirasak Rirksomboon[a]

[a] The Petroleum and Petrochemical College, and Center for Petroleum, Petrochemicals and Advanced Materials, Chulalongkorn University, Bangkok 10330, Thailand
[b] Centre for Advanced Materials and Environmental Research, Mahanakorn University of Technology, Bangkok 10530, Thailand

ARTICLE INFO

Article history:
Available online 13 November 2010

Keywords:
H_2 production
Steam reforming
Bio-oils
$Ce_{0.75}Zr_{0.25}O_2$

ABSTRACT

The Ni metallic phase supported metal oxides such as α-Al_2O_3, $Ce_{0.75}Zr_{0.25}O_2$, and MgO were tested under the steam reforming of acetic acid selected as a representative compound for the aqueous phase of the bio-oil derived from biomass pyrolysis. It was found that the catalytic activity and carbon formation for the catalysts studied were significantly dependent on the Ni content and the nature of support. The 15%Ni/$Ce_{0.75}Zr_{0.25}O_2$ catalyst exhibited the highest catalytic performance in terms of C–C breakage conversion and hydrogen yield. In addition, the redox property of $Ce_{0.75}Zr_{0.25}O_2$ provided higher stability than the MgO and α-Al_2O_3 due to its less carbon deposition even at low steam-to-carbon ratios.

1. Introduction

Hydrogen is being considered as an environmentally friendly source of energy for power generation with fuel cells. Currently, hydrogen is produced from fossil fuels such as natural gas, naphtha and coal [1]. However, these resources utilized result in a large quantity of greenhouse gas emission. For this reason, a renewable energy source such as biomass may be used as an alternative feedstock because it appears to have formidably positive environmental properties resulting from no net releases of carbon dioxide (CO_2) and very low sulfur content [2]. Biomass can be converted to bio-oils by fast pyrolysis and then the bio-oils can be converted to hydrogen (H_2) by catalytic steam reforming [3–5].

Bio-oils produced from biomass pyrolysis are virtually separated into the oil and water-rich phases. The oil phase contains lignin-derived materials that can be used for the production of more valuable products while the water-rich phase contains mostly carbohydrate-derived compounds that can be catalytically reformed with steam [6–8]. Since acetic acid is one of the major components of the water-rich phase of bio-oil [5,9], therefore, steam reforming (SR) of acetic acid has been extensively investigated as a model reaction in order to understand the integrity required for designing the efficient catalysts for use in the SR of the bio-oil water-rich phase.

Ni based catalysts are intensively used for steam reforming of hydrocarbons including oxygenate hydrocarbons [10–12]. It was reported the major problem of a Ni-based catayst is its fast deactivation due to carbon deposition and/or metal sintering [13,14]. Alternative supports such as dolomite, olivine, MgO and MgO–CaO were reported to improve the catalytic stability [15–17]. Recently, it has been reported that $Ce_{1-x}Zr_xO_2$ mixed oxides exhibited a superior resistance to carbon formation on the partial oxidation and steam reforming of hydrocarbons [18,19], due to the high oxygen vacancy and oxygen mobility. In our early study, we have also found that $Ce_{0.75}Zr_{0.25}O_2$ solid solution exhibited the highest reducibility and activity for oxidation reactions [18–20]. In this study, we investigate the effect of the supports on the steam reforming catalytic activity and stability of acetic acid as a biomass-derived oxygenate compound model over Ni/$Ce_{0.75}Zr_{0.25}O_2$, Ni/α-Al_2O_3 and Ni/MgO catalysts.

2. Experimental

2.1. Catalyst preparation and characterizations

$Ce_{0.75}Zr_{0.25}O_2$ and MgO were prepared via urea hydrolysis and precipitation method, respectively, whereas α-Al_2O_3 was obtained from a company. $Ni(NO_3)_2$ aqueous solution as Ni precursors was incorporated into the supports by the impregnation method. The desired amounts of Ni loading were 5–25 wt% for $Ce_{0.75}Zr_{0.25}O_2$, and 15 wt% for both MgO and α-Al_2O_3. The catalysts were characterized by BET, XRD, TPR, TPO, and TEM techniques. The detailed synthesis procedure and characteristics of catalysts were reported elsewhere [19].

2.2. Catalytic activity testing

To compare the catalytic activity and stability of the catalysts on the steam reforming of acetic acid, the reaction was carried out at 650 °C with steam-to-carbon (S/C) ratios ranging from 1 to 6.

* Corresponding author. Tel.: +66 0 2988 3655x2325; fax: +66 0 2988 4039.
E-mail address: vissanu@mut.ac.th (V. Meeyoo).

0920-5861/$ – see front matter.
doi:10.1016/j.cattod.2010.10.054

Typically, 0.1 g of catalyst was packed between the layers of quartz wool in a quartz tube microreactor (i.d. 10 mm) placed in an electric furnace equipped with K-type thermocouples. The temperature of catalyst bed was monitored and controlled using Shinko temperature controllers. A liquid mixture feed consisting of a known composition of acetic acid aqueous solution was introduced into an evaporator at ca. 140 °C to vaporize and mix with a gas stream prior to entering the reactor set at a desired temperature. Gaseous products were analyzed using on-line gas chromatographs in series equipped with TCD and FID detectors. Prior to running the reaction, the catalyst was reduced *in situ* with a flow of 50% H_2 in N_2 gas at 600 °C for 2 h. The C–C breakage conversion of acetic acid was defined as a molar ratio of the gaseous single carbon compounds (CH_4, CO and CO_2) in the product steam to the acetic acid reactant and the product yield was defined as a molar ratio of the product to the theoretical amount of product produced from steam reforming of acetic acid. The C–C breakage conversion and product yield reported in this work were calculated as follows:

$$\text{C} - \text{C breakage conversion}\,(\%) = \frac{\text{mol}_{CH_4,\text{out}} + \text{mol}_{CO,\text{out}} + \text{mol}_{CO_2,\text{out}}}{2 \times \text{mol}_{AcOH,\text{out}}} \times 100 \quad (1)$$

$$\%\ \text{yield}_{H_2} = \frac{\text{mol}_{H_2,\text{out}}}{4 \times \text{mol}_{AcOH,\text{in}}} \times 100 \quad (2)$$

$$\%\ \text{yield}_{CO} = \frac{\text{mol}_{CO,\text{out}}}{2 \times \text{mol}_{AcOH,\text{in}}} \times 100 \quad (3)$$

$$\%\ \text{yield}_{CO_2} = \frac{\text{mol}_{CO_2,\text{out}}}{2 \times \text{mol}_{AcOH,\text{in}}} \times 100 \quad (4)$$

$$\%\ \text{yield}_{CH_4} = \frac{\text{mol}_{CH_4,\text{out}}}{2 \times \text{mol}_{AcOH,\text{in}}} \times 100 \quad (5)$$

3. Results and discussion

3.1. Catalyst characterization

The BET surface areas, degrees of metal dispersion, and mean size diameters of the catalysts are shown in Table 1. As for the $Ni/Ce_{0.75}Zr_{0.25}O_2$ catalysts, their surface areas are in the range of 58–78 m^2/g and decreased with increasing Ni loading. At a given support, the degree of metal dispersion is decreased and the mean size diameter is increased as the Ni loading is increased. This is due to the formation of NiO bulk particles [19]. However, at a given Ni loading (15 wt%), the $Ni/Ce_{0.75}Zr_{0.25}O_2$ catalyst possesses the highest metal dispersion degree with the smallest mean size diameter. The low metal dispersion degree of 15%Ni/α-Al_2O_3 is due to the low surface area of the support while that of 15%Ni/MgO is owed to the formation of NiO–MgO solid solution.

The XRD patterns of the $Ni/Ce_{0.75}Zr_{0.25}O_2$ catalysts indicate a typical cubic fluorite structure of ceria with the presence of NiO phase (37°, 43°, and 62° (2θ)) as shown in Fig. 1. However, the Ni or NiO phase was absent in the case of low Ni loading (5 wt%). Since the peak intensity was amplified with increasing Ni loading, it was suggested that NiO species is present in the forms of nano-particles and bulk agglomerated particles at a low- and a high-Ni content, respectively [19]. This result appears to be in good agreement with the data on degree of metal dispersion. Furthermore, the XRD pattern of the 15%Ni/α-Al_2O_3 catalyst reveals the separate phases of NiO and α-Al_2O_3, yet the absence of Ni–Al alloy phase. However, that of the 15%Ni/MgO catalyst indicates a NiO–MgO solid solution as similar to what reported elsewhere [21].

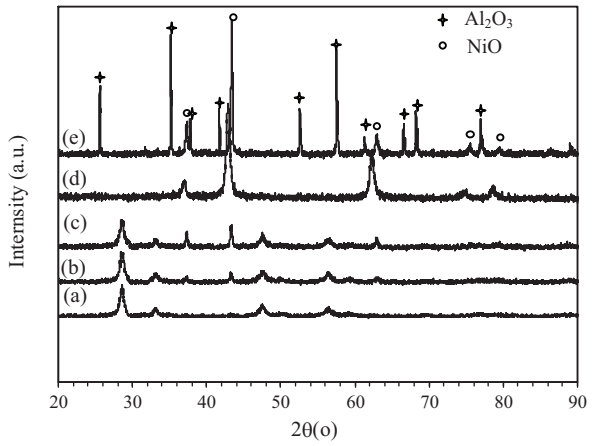

Fig. 1. XRD patterns for the catalysts investigated (a) 5%$Ni/Ce_{0.75}Zr_{0.25}O_2$, (b) 15%$Ni/Ce_{0.75}Zr_{0.25}O_2$, (c) 25%$Ni/Ce_{0.75}Zr_{0.25}O_2$, (d) 15%Ni/MgO, and (e) 15%Ni/α-Al_2O_3.

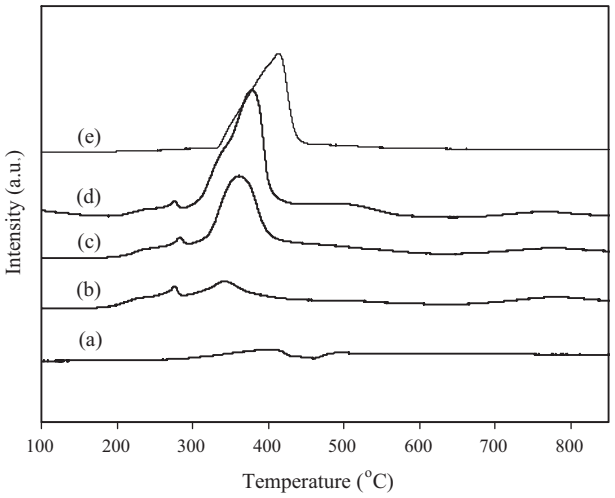

Fig. 2. H_2-TPR profiles for the catalysts with a heating rate of 10 °C/min, a reducing gas containing 5% H_2 in N_2 with a flow rate of 30 ml/min: (a) 15%Ni/MgO, (b) 5%$Ni/Ce_{0.75}Zr_{0.25}O_2$, (c) 15%$Ni/Ce_{0.75}Zr_{0.25}O_2$, (d) 25%$Ni/Ce_{0.75}Zr_{0.25}O_2$, and (e) 15%Ni/α-Al_2O_3.

Fig. 2 depicts the H_2-TPR profiles for $Ni/Ce_{0.75}Zr_{0.25}O_2$, Ni/α-Al_2O_3 and Ni/MgO. The results showed that the reducibility

Table 1
BET surface area, degree of metal dispersion and mean size diameter of the catalysts.

Catalyst	BET surface area (m^2/g)	Degree of metal dispersion (%)	Mean size diameter[a] (nm)	Mean size diameter[b] (nm)
5%$Ni/Ce_{0.75}Zr_{0.25}O_2$	78	8.29	–	12.2
15%$Ni/Ce_{0.75}Zr_{0.25}O_2$	68	3.06	29.5	33.0
25%$Ni/Ce_{0.75}Zr_{0.25}O_2$	58	2.15	44.7	47.0
15%Ni/Al_2O_3	4	1.98	47.6	51.0
15%Ni/MgO	50	2.11	–	47.8

[a] Calculated from XRD.
[b] Calculated from H_2-chemisorption.

of the 15 wt% Ni loading catalysts is in the following order: $Ni/Ce_{0.75}Zr_{0.25}O_2 > Ni/\alpha\text{-}Al_2O_3 > Ni/MgO$. Noticeably, two H_2 consumption peaks are observed for $Ni/Ce_{0.75}Zr_{0.25}O_2$ catalyst as compared with that for $Ni/\alpha\text{-}Al_2O_3$ catalyst. The low temperature peak in the range of 250–300 °C can be associated with the reduction of free NiO particles and the other peak in the range of 300–450 °C can be attributed to the reduction of complex NiO species in intimate contact with the oxide supports [19,22,23]. This suggests that interaction between Ni and the $Ce_{0.75}Zr_{0.25}O_2$ support makes the catalysts more reducible, which probably enhances the oxygen mobility during the reforming reaction. For the $Ni/\alpha\text{-}Al_2O_3$ catalyst, only one broad peak attributed to agglomerated Ni is observed at ca. 410 °C. Similar reduction patterns were found in the cases of 5 and 25 wt% Ni loadings on $Ce_{0.75}Zr_{0.25}O_2$ with slightly lower reduction temperatures. It should be noted that the absence of the reduction peak for 15%Ni/MgO catalyst might be due to the incorporation of NiO into the MgO lattice resulting in the formation of NiO–MgO solid solution [21,24].

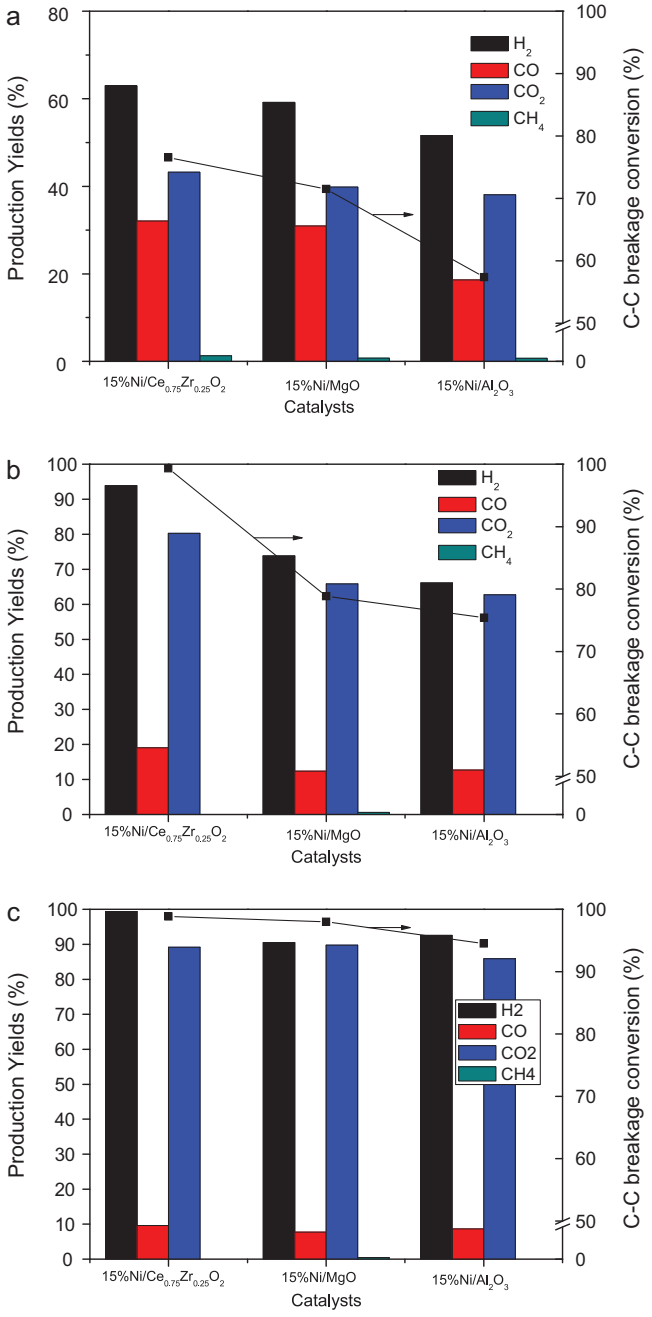

Fig. 3. Effect of S/C ratio on the C–C breakage conversion, the yields of carbon containing products and hydrogen yield over: $15\%Ni/Ce_{0.75}Zr_{0.25}O_2$, 15%Ni/MgO and $15\%Ni/\alpha\text{-}Al_2O_3$ at 650 °C and S/C ratio: (a) 1, (b) 3 and (c) 6.

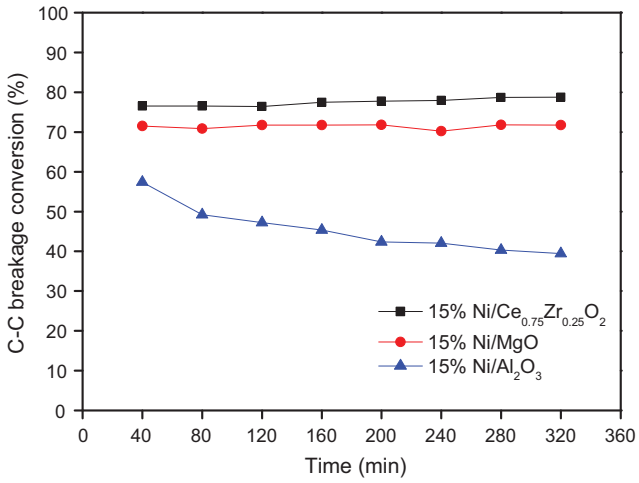

Fig. 4. Catalytic activity for acetic acid steam reforming over $15\%Ni/Ce_{0.75}Zr_{0.25}O_2$, $15\%Ni/\alpha\text{-}Al_2O_3$, and 15%Ni/MgO catalysts: $T = 650$ °C and S/C ratio = 1.

3.2. Catalytic activity for acetic acid steam reforming

To investigate the effect of support on the catalytic activity and stability, the $\alpha\text{-}Al_2O_3$ (inert) and MgO (basic support) were selected to compare with $Ce_{0.75}Zr_{0.25}O_2$ support for steam reforming of acetic acid. The performance of the catalyst was defined in terms of C–C breakage conversion and hydrogen yield. The results showed that the $15\%Ni/Ce_{0.75}Zr_{0.25}O_2$ was the most active catalyst while the $15\%Ni/\alpha\text{-}Al_2O_3$ was the least active one for such a steam reforming reaction as shown in Fig. 3. This could be in part ascribed to the nature of supports steering different degrees of metal dispersion in which these were 3.06, 2.11, and 1.98% for $15\%Ni/Ce_{0.75}Zr_{0.25}O_2$, 15%Ni/MgO and $15\%Ni/\alpha\text{-}Al_2O_3$, respectively. It should be noted that for $15\%Ni/\alpha\text{-}Al_2O_3$, the catalytic activity was solely due to Ni metal.

During the course of our experiments H_2 and CO_2 were not only the steam reforming products found, CO and a trace of CH_4 were detected at low steam to carbon ratio (S/C = 1). It was reported CO could be generated from ketene decomposition [25] as shown in

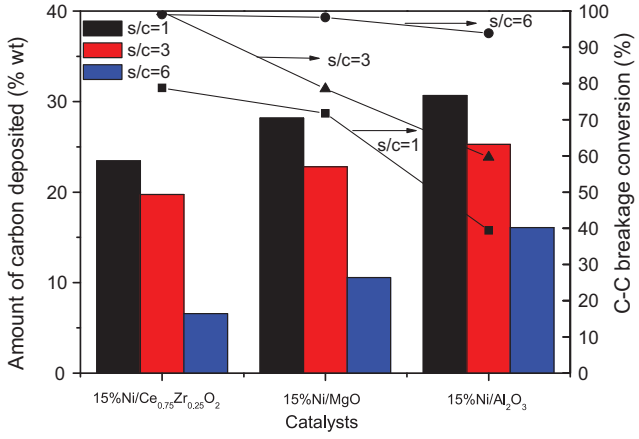

Fig. 5. Total amount of carbon deposited on catalysts via acetic acid steam reforming over $15\%Ni/Ce_{0.75}Zr_{0.25}O_2$, 15%Ni/MgO and $15\%Ni/\alpha\text{-}Al_2O_3$ catalysts; after 320 min on stream, at 650 °C, S/C ratios of 1–6.

Table 2
Acetic acid steam reforming on 0.1 g of 5%Ni/$Ce_{0.75}Zr_{0.25}O_2$, 15%Ni/$Ce_{0.75}Zr_{0.25}O_2$ and 25%Ni/$Ce_{0.75}Zr_{0.25}O_2$ catalysts at T = 650 °C and WHSV (HAc) = 22 h^{-1}.

Catalyst	S/C ratio	Yield* (%)				C–C breakage conversion* (%)
		H_2	CO	CO_2	CH_4	
5%Ni/$Ce_{0.75}Zr_{0.25}O_2$	1	33.84	15.78	22.52	0.00	38.29
	3	64.39	10.89	57.55	0.00	68.44
	6	98.52	8.46	90.53	0.00	98.98
15%Ni/$Ce_{0.75}Zr_{0.25}O_2$	1	62.98	32.06	43.20	1.30	76.56
	3	93.83	19.10	80.25	0.00	99.35
	6	99.34	9.59	89.15	0.00	98.84
25%Ni/$Ce_{0.75}Zr_{0.25}O_2$	1	60.66	30.69	41.35	0.84	72.88
	3	73.62	11.65	65.44	0.00	77.09
	6	98.74	9.31	89.43	0.00	98.74

* At time on steam of 40 min.

Eqs. (6) and (7). The absence of C_2H_4 in this case would be, then, suggested that CO is probably produced via the decomposition of acetic acid (Eq. (8)) as reported elsewhere [25] or from the reverse water gas shift reaction [12]. Since the methanation reaction is not thermodynamically favoured under our conditions, CH_4 might be generated from the decarboxylation of acetic acid (Eq. (9)) [12].

$$CH_3COOH \rightarrow CH_2CO + H_2O \quad (6)$$

$$2CH_2CO \rightarrow C_2H_4 + 2CO \quad (7)$$

$$CH_3COOH \rightarrow 2CO + 2H_2 \quad (8)$$

$$CH_3COOH \leftrightarrow CH_4 + CO_2 \quad (9)$$

The results also showed that the hydrogen yield increases steadily with the increase in steam to carbon ratio, in parallel with the carbon dioxide concentration, due to the shift in the water gas shift equilibrium toward hydrogen production. The absence of methane in the cases of S/C = 3 and 6 for 15%Ni/$Ce_{0.75}Zr_{0.25}O_2$, and 15%Ni/α-Al_2O_3 catalysts might be due to the steam reforming reaction of methane. However, a trace amount of CH_4 was still observed on the 15%Ni/MgO catalyst at S/C ratios of 3 and 6, which might be due to the presence of NiO–MgO solid solution.

The effect of Ni loading on the $Ce_{0.75}Zr_{0.25}O_2$ support was further investigated. It was found that the catalytic activity at a low S/C ratio was dependent on the nickel loading as shown in Table 2. The optimal loading was 15 wt%, which is related to the metal surface area and the metal particle size. At a high steam to carbon ratio (S/C = 6), the effect of Ni loading seems to be less pronounced.

3.3. Carbon formation

The results showed that the C–C breakage conversion of 15%Ni/α-Al_2O_3 decreases from 57% to 39% while those of 15%Ni/$Ce_{0.75}Zr_{0.25}O_2$ and 15%Ni/MgO are rather stable, reported at 76% and 71%, respectively (at S/C = 1) as shown in Fig. 4. This suggests that 15%Ni/$Ce_{0.75}Zr_{0.25}O_2$ and 15%Ni/MgO are more

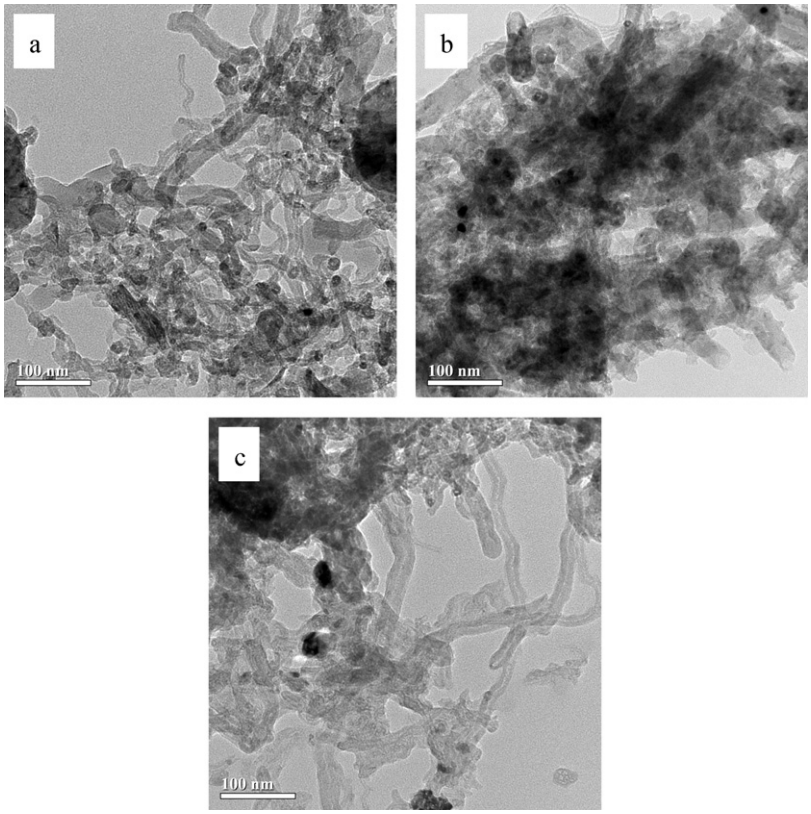

Fig. 6. TEM images of the spent catalysts: (a) 15%Ni/α-Al_2O_3, (b) 15%Ni/$Ce_{0.75}Zr_{0.25}O_2$, and (c) 15%Ni/MgO.

active and stable than 15%Ni/α-Al_2O_3. It is noticed that although 15%Ni/α-Al_2O_3 shows the lowest C–C breakage conversion, the amount of carbon formed is somewhat higher than that of 15%Ni/$Ce_{0.75}Zr_{0.25}O_2$ and 15%Ni/MgO (Fig. 5). At higher S/C ratios (S/C = 3 and 6), the 15%Ni/$Ce_{0.75}Zr_{0.25}O_2$ exhibits a better activity with less carbon formation as compared to 15%Ni/MgO and 15%Ni/α-Al_2O_3. This indicates that the synergetic effect of an ease of reducibility and a good oxidation ability of the $Ce_{0.75}Zr_{0.25}O_2$ mixed oxide could promote the oxidation of carbon precursors on the nickel surface as similar to what reported elsewhere [19,26]. The spent catalysts were found to be covered with filamentous carbons as shown in Fig. 6 and the results comform to the TPO analysis, which indicated mainly a high temperature oxidation peak at ca. 650 °C (the results are not shown).

4. Conclusions

It can be concluded that the nature of the support affects the catalytic activity and stability by influencing the metal degree of dispersion and water activation. The $Ce_{0.75}Zr_{0.25}O_2$ supported catalysts exhibit an excellent activity and stability for an acetic acid steam reforming. This is due to good redox properties and oxygen mobility of $Ce_{0.75}Zr_{0.25}O_2$, promoting the oxidation of carbon species. At a high steam to carbon ratio (S/C = 6), the effect of the support on the activity was found to be less pronounced but was still present on the carbon formation of the catalysts.

Acknowledgements

This work was supported by the Thailand Research Fund (under Waste-to-Energy project and Royal Golden Jubilee Ph.D. Program: Grant 0170/46), National Metal and Materials Technology Center (Project No. MT-B-50-END-74-038-G), and the Sustainable Petroleum and Petrochemicals Research Unit under the National Center of Excellence for Petroleum, Petrochemicals, and Advanced Materials, Chulalongkorn University.

References

[1] M.A. Peña, J.L.G. Gómez, J.L.G. Fierro, Appl. Catal. A: Gen. 144 (1996) 7–57.
[2] R.C. Saxena, D.K. Adhikari, H.B. Goyal, Renew. Sustainable Energy Rev. 13 (2009) 167–178.
[3] S. Czernik, R. Evans, R. French, Catal. Today 129 (2007) 265–268.
[4] K. Takanabe, K. Aika, K. Inazu, T. Baba, K. Seshan, L. Lefferts, J. Catal. 243 (2006) 263–269.
[5] S. Zhang, Y. Yan, T. Li, Z. Ren, Bioresour. Technol. 96 (2005) 545–550.
[6] S.S. Kelley, X.-M. Wang, M.D. Myers, D.K. Johnsom, J.W. Scahill, in: A.V. Bridgwater, D.G.B. Boocock (Eds.), Developments in Thermochemical Biomass Conversion, Blackie Academic & Profesional, London, 1997, p. 557.
[7] J. Shabtai, W. Zmierczak, E. Chomet, in: R.P. Overend, E. Chornet (Eds.), Making a Business from Biomass in Energy, Environment, Chemicals, Fibers, and Materials, vol. 2, Pergamnon, Oxford, 1997, p. 1037.
[8] C. Jindarom, V. Meeyoo, T. Rirksomboon, P. Rangsunvigit, Chemosphere 67 (2007) 1384–1477.
[9] F. Bimbela, M. Oliva, J. Ruiz, L. García, J. Arauzo, J. Anal. Appl. Pyrolysis 79 (2007) 112–120.
[10] A.J. Vizcaíno, P. Arena, G. Baronetti, A. Carrero, J.A. Calles, M.A. Laborde, N. Amadeo, Int. J. Hydrogen Energy 33 (2008) 3489–3492.
[11] X. Hu, G. Lu, J. Mol. Catal. A: Chem. 261 (2007) 43–48.
[12] D. Wang, D. Montané, E. Chornet, Appl. Catal. A: Gen. 143 (1996) 245–270.
[13] L. Garcia, R. French, S. Czernik, E. Chomet, Appl. Catal. A: Gen. 201 (2000) 225–239.
[14] E.G. Baker, L.K.M.D. Brown, Ind. Eng. Chem. Res. 26 (1987) 1335–1339.
[15] K. Sato, K. Fujimoto, Catal. Commun. 8 (2007) 1697–1701.
[16] D. Swierczynski, S. Libs, C. Courson, A. Kiennemann, Appl. Catal. B: Environ. 74 (2007) 211–222.
[17] T. Miyazawa, T. Kimura, J. Nishikawa, S. Kado, K. Kunimori, K. Tomishige, Catal. Today 115 (2006) 254–262.
[18] A. Bampenrat, V. Meeyoo, B. Kitiyanan, P. Rangsunvigit, T. Rirksomboon, Appl. Catal. A: Gen. 373 (2010) 154–159.
[19] S. Pengpanich, V. Meeyoo, T. Rirksomboon, Catal. Today 93–95 (2004) 95–105.
[20] M. Thammachart, V. Meeyoo, T. Risksomboon, S. Osuwan, Catal. Today 68 (2001) 53–61.
[21] J. Barbero, M.A. Peña, J.M. Campos-Martin, J.L.G. Fierro, P.L. Arias, Catal. Lett. 87 (2003) 211–218.
[22] H. Roh, K. Jun, W. Dong, J. Chang, S. Park, Y. Joe, J. Mol. Catal. A: Chem. 181 (2002) 137–142.
[23] J.A. Montoya, E. Romero-Pascual, C. Gimon, P. Del Angle, A. Monzon, Catal. Today 63 (2000) 71–85.
[24] Y. He Wang, H. Mei Liu, B. Qing Xu, Catal. A. 299 (2009) 44–52.
[25] A.C. Basagiannis, X.E. Verykios, Int. J. Hydrogen Energy 32 (2007) 3343–3355.
[26] P. Biswas, D. Kunzru, Int. J. Hydrogen Energy 32 (2007) 969–980.